Mechanistic Study of the Addition of Pyruvate to NAD^+ Catalyzed by Lactate Dehydrogenase†

John W. Burgner II* and William J. Ray, Jr.

ABSTRACT: The binary complex of NAD^+ and dogfish A_4 lactate dehydrogenase reacts reversibly with pyruvate enol to produce an inactive, enzyme·adduct complex, in which the nicotinamide and pyruvate moieties are linked by means of a covalent bond. This process is examined in both the forward and reverse directions as a function of reactant and buffer concentrations at pH 7, under conditions where the enolization of pyruvate is at equilibrium, and the involvement of complexes with stoichiometry E·NAD, E·NAD·Pyr_E, and E·NAD·Pyr_K is defined. (The subscripts, E and K, indicate the enol and keto forms of pyruvate.) One pathway for formation of the adduct complex involves the prior formation of the E·NAD·Pyr_E complex from E·NAD and pyruvate enol; the alternative pathway involves formation of the same complex via the enolization of E·NAD·Pyr_K, a process that is catalyzed by an *external* (nonenzymic) base. The possible use of the adduct reaction as a model for the normal enzymic reaction is considered.

The inhibition of the normal enzymic reaction of lactate dehydrogenase (LDH),[1] which occurs at high pyruvate concentrations or upon treatment of the enzyme with NAD^+ and pyruvate, has been attributed to the slow formation of a tightly bound, abortive, binary complex, E·adduct, whose properties contrast with those of the loose, rapidly formed, ternary complex, E·NAD·Pyr. The possible physiological importance of the adduct complex has been considered in some detail (cf. Burgner et al., 1978). However, recognition that the adduct reaction might serve as a useful model for the normal enzymic reaction (oxidation of lactate by NAD to pyruvate and NADH) is not widespread. The present study considers the mechanism for the forward and reverse adduct reactions[2] from this standpoint.

The reaction (Scheme I) between NAD^+ and pyruvate, both

SCHEME I: The Reaction of Pyruvate Enol with NAD.

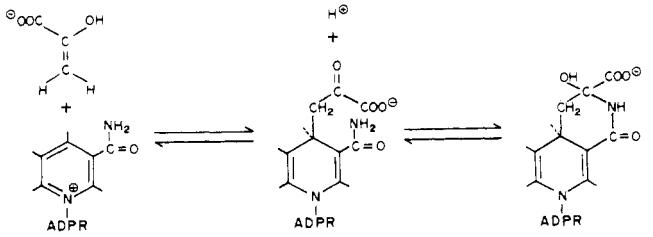

I II III

in the presence of LDH at near neutral pH as well as in the absence of the enzyme at high pH, involves the formation of a covalent bond between the A side of the C_4 position in nicotinamide and the β carbon of pyruvate to give I (attack at the B side also occurs in the nonenzymic reaction); in addition, during the nonenzymic (base-catalyzed) reaction, a bond subsequently forms between the amide nitrogen and the pyruvate carbonyl carbon to give II (DiSabato, 1968; Everse et al., 1971b). The latter reaction also occurs when the adduct is formed in the presence of the enzyme at pH 10 but probably only after dissociation of the adduct from the enzyme (Arnold & Kaplan, 1974).

A detailed consideration of possible mechanisms for the enzyme-catalyzed reaction of NAD and pyruvate must take into account the following conclusions and suggestions from previous studies: (a) the enol form of pyruvate is one of the reactants (Burgner & Ray, 1974); (b) at "high" pyruvate/enzyme ratios, the reaction is in steady state, relative to the enol, for most of its course (Burgner & Ray, 1974; see also the Results); (c) the enzyme-bound form of NAD^+ is the other reactant (Griffin & Criddle, 1970; Sugrobova et al., 1972); (d) the reactive E·NAD complex is predominantly in the tetrameric form (Sugrobova et al., 1972; Burgner & Ray, 1974); (e) the four coenzyme binding sites of LDH are equal and independent (Holbrook & Gutfreund, 1973; Burgner, 1973). Additional complexes E·NAD·Pyr_E and E·NAD·Pyr_K (Novoa et al., 1959; Burgner, 1973; Burgner & Ray, 1974; Burgner et al., 1978) also must be considered. Other steps that could affect the overall process are the direct dissociation of bound adduct (k_7, below) and the buffer catalyzed interconversion (tautomerization) of enzyme-bound forms of pyruvate enol and ketone (k_3 and k_4, below). All of these complexes and steps are combined in Scheme II to provide a basis for interpreting

SCHEME II[a]

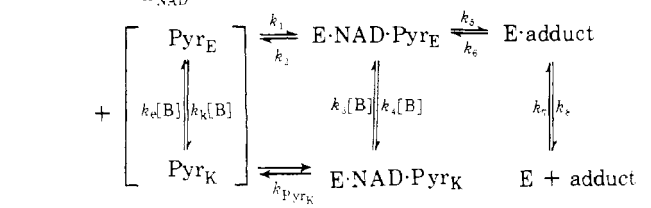

[a] In this scheme, $k_2/k_1 = K_{PyrE}$, $k_e/k_k = K_{enol}$, and $K_{eq} = k_5K_{enol}/k_6K_{PyrE}$; B refers to buffer without respect to differences in the acidic and basic forms.

† From the Department of Biological Sciences, Purdue University, West Lafayette, Indiana 47907. *Received August 30, 1977.* This investigation was supported by a research grant from the National Science Foundation (GB 7500480).

[1] Abbreviations and symbols used: LDH, lactate dehydrogenase (the dogfish A_4 enzyme unless otherwise specified); E, a subunit of an LDH tetramer; Pyr, pyruvate; Pyr_E and Pyr_K, the enol and keto forms of pyruvate, respectively; NAD–Pyr or adduct, the covalent addition product or products of NAD and pyruvate (see I); equilibrium dissociation constants are designated by K.

[2] The "reverse" adduct reaction refers to the process, E·adduct → E·NAD·Pyr_E → E·NAD + Pyr; the "decomposition of the adduct complex" (see below) refers to the sum of the above process and E·adduct (+ NAD) → E·NAD + adduct, viz., where the precise fate of the adduct complex is not specified.

0006-2960/78/0417-1654$01.00/0

the effect of the pyruvate, NAD, and buffer (imidazole) concentrations on both the forward and reverse adduct reactions. The involvement of hydrogen ions will be considered in a subsequent paper.

Although Scheme II is more complex than the scheme used previously for an analysis of the adduct reaction under a more limited set of conditions (Burgner & Ray, 1974), the rate equation for Scheme II reduces to that used previously when those conditions were imposed; see the Appendix.

Experimental Section

Materials

Grade III samples of dithiothreitol, oxamic acid, oxalic acid, and sodium pyruvate (Sigma), potassium pyruvate (Nutritional Biochemicals), and NAD, NADH, and APAD (P-L Biochemicals) were used without further purification; solutions of these were prepared and adjusted to pH just before use. Dogfish A_4 LDH was prepared either by the method of Wassarman & Lentz (1971) or by use of a cibracon blue agarose affinity column (unpublished procedure, Szymanski, E. S., & Burgner, J. W., II, 1976). Its activity by the standard assay always was at least 95% of the reported maximum for the dogfish enzyme (Burgner & Ray, 1974). Pig B_4 LDH was purchased from Sigma, but was used only where specified. Both enzymes were stored at 4 °C as ammonium sulfate suspensions, and stock solutions were prepared by dialysis against the appropriate buffer (containing 1×10^{-4} M dithiothreitol) at 4 °C just before use.

Methods

Adduct Reaction. The rate and extent of the adduct reaction, as a function of the reactant and buffer concentrations, were measured either by following the appearance of an absorption band at 325 nm with a Cary 15 or Perkin-Elmer 575 spectrophotometer or by following the disappearance of the tryptophan fluorescence of the enzyme with a combination grating-filter fluorometer. The fluorometer was constructed from a Zeiss monochrometer and deuterium light source (which provided excitation radiation at 295 nm), a C-51 Corning filter (to select the emission radiation), an Aminco blank-subtract fluorometer, and a Honeywell 19 K recorder. The appropriate concentrations of reactants, dithiothreitol, and buffer were preequilibrated at 15 °C in a water-cooled cell holder, and the appropriate quantity of enzyme (at the same temperature) was added to initiate the enzymic reaction. For the nonenzymic reaction, pyruvate was used to initiate the process, which was conducted under conditions similar to those above. Corrections for reactant dilution (≤2% in most cases) were made when necessary.

Decomposition[2] *of the Adduct Complex.* The adduct complex was prepared by incubating a mixture of enzyme, NAD (4 mM), pyruvate (20 mM), and imidazole buffer (0.3 M, pH 7) for approximately 1 h at 15 °C. An activity assay was used to estimate the stoichiometry of the final product (Burgner et al., 1978); typically, >90% conversion to E·adduct was obtained. For the decomposition reaction, a small aliquot (10 to 20 μL) of the solution was added to 2 mL of a solution containing NAD (2×10^{-4} M), potassium oxalate (0.1 M), and the appropriate buffer concentration; in some cases, potassium oxalate was not included. The assays were monitored by the same procedures used for the forward reaction.

Numerical Methods. Reduction of the data involving optical densities was accomplished by means of the same procedures discussed previously (Burgner & Ray, 1974). Reduction of the fluorescence data to a linear form (see Results section) was conducted with an HP-65 calculator and a program based on the method of Holbrook (1972). The reduced data were used to obtain estimates of the rate constants in equations for various reaction schemes by using the numerical methods and programs described previously (Burgner & Ray, 1974), together with an additional program (SPSS21 from the Purdue University Computer Center) for nonlinear regression analysis in situations where the residual minimum is shallow. To provide initial estimates for such analyses, graphical solutions or approximations were applied to the data; data were discarded if the best-fit estimates deviated by more than 50% from the initial estimates.

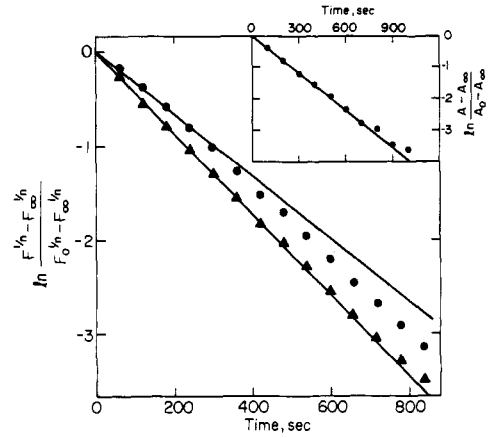

FIGURE 1: A semilog plot for the first-order decomposition of E·adduct using the fluorescence of enzyme tryptophan, either directly or after transformation. The increase in fluorescence was recorded at 15 °C for a reaction mixture in a 1 × 1 cm fluorescence cell that initially contained 1.4×10^{-7} M E·adduct, 2×10^{-4} M NAD, 0.1 M potassium oxalate, and 0.3 imidazole·HCl; the final reaction pH was 6.91. Plot using the observed fluorescence, F (●); plot using transformed fluorescence, $F^{1/n}$, with $n = 4$ (▲). The upper solid line was drawn by eye; to emphasize the curvature in the plot, the lower line was drawn on the basis of an estimate for K_{obsd} of 4.3×10^{-3} s^{-1}. (Inset) A semilog plot for the decomposition of E·adduct using absorbance. The absorption band at 325 nm was followed under the same conditions as above, with the exception that the system initially contained 5×10^{-6} M E·adduct, 4×10^{-4} M NAD, and 2×10^{-3} M pyruvate. The solid line was drawn on the basis of an estimate for k_{obsd} of 4.0×10^{-3} s^{-1} (see Results section).

Results

Quenching of Tryptophan Fluorescence in the Enzyme–Adduct Complex. The fluorescence of the tryptophans in the LDH isozymes, A_4 (dogfish) and B_4 (pig), is substantially quenched by the presence of bound adduct. This effect can serve as the basis of a procedure for following the adduct reaction at enzyme concentrations much lower than can be used in procedures based on absorbance measurements, if the relationship between tryptophan fluorescence and the stochiometry of the adduct complex can be established. The required relationship can be determined by following the fluorescence changes that accompany the decomposition of the adduct complex (the decomposition can be followed more accurately than adduct formation), since the decomposition is known to be a first-order process with respect to the adduct complex on the basis of absorbance changes that occur during the same process; see Figure 1, inset. In these calibration experiments, potassium oxalate is used to drive the decomposition to completion (by formation of the E·NAD·oxalate complex), because neither NAD, nor oxalate, nor a combination of these substantially absorbs at 325 nm nor quenches tryptophan fluorescence when bound to the enzyme (at pH 7). The data (●, Figure 1) show that the change in tryptophan fluorescence as a function of time is not that expected for a first-order pro-

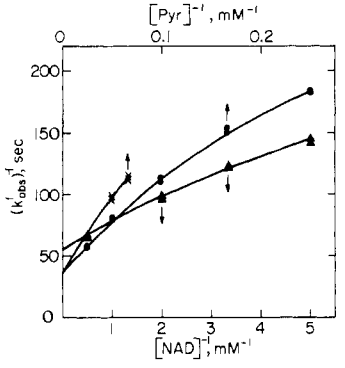

FIGURE 2: The effect of NAD and pyruvate concentration on the observed rate constant for the adduct reaction in the forward direction. Values for rate constants were estimated from curves such as those in Figure 1 for $n = 4$ (see Methods and Results section). The reaction mixture initially contained NAD and potassium pyruvate, and the concentration of the nonvaried member of the reactant pair was 5×10^{-4} M NAD (■), 1×10^{-3} M NAD (●), and 0.02 M pyruvate (▲). The enzyme concentration varied from 0.2 μM at low reactant concentration to 0.6 μM at high levels. Other conditions are the same as those in Figure 1. Each point represents the average of two determinations, and the solid lines are drawn by using eq 3 and values for k_f, 1.0 M^{-1} s^{-1}, k_r, 2.3×10^{-3} s^{-1}, K_{PyrK}, 0.013 M, K_{NAD}, 1.3×10^{-3} M, and K_{enol}, 4×10^{-6}.

cess at four identical and noninteracting sites of a tetramer. Thus, tryptophan fluorescence, as opposed to adduct absorbance in the E·adduct complex, is a nonlinear function of site occupancy by the adduct in the dogfish A_4 isozyme. Similar experiments with pig B_4 LDH provide analogous conclusions, both with respect to NADH binding (Holbrook, 1972) as well as formation of the adduct complex (not shown). In order to correct for the nonlinear relationship between fluorescence and site occupancy (at constant enzyme concentration), Holbrook's approximation, site occupancy $\alpha F^{-1/n}$ where n is a constant (Holbrook, 1972), is used. Thus, tryptophan fluorescence at a specified reaction time should be described by eq 1 when site occupancy is varied (decreased) in a first-order process. Here, F is the fluorescence intensity, and the subscripts 0, t, and ∞ refer to reaction times.

$$\ln \frac{F_t^{1/n} - F_\infty^{1/n}}{F_0^{1/n} - F_\infty^{1/n}} = -kt \qquad (1)$$

A computer-assisted fitting procedure was used to adjust the value of n in eq 1 so that its left-hand side becomes linear with time when the experimental values of F are inserted: $n = 4$ (Figure 1, Δ). The close similarity between the value of the rate constant for decomposition of the adduct complex, obtained from the slope of this plot (4.3×10^{-3} s^{-1}), and that obtained from absorbance measurements (4.0×10^{-3} s^{-1}; inset, Figure 1)—where the change in absorbance is directly proportional to site occupancy—substantiates this approach. Hence, the relationship site-occupancy $\alpha F^{-1/4}$ is used, throughout, to follow both the forward and reverse adduct reactions when the concentration of LDH is less than 5×10^{-6} in total sites.

The Pre-Steady-State Burst in the Absence of Buffer. At low concentrations of imidazole (<0.005 M, pH 7) as well as at low enzyme concentration, product-time curves for the (forward) adduct reaction with both the pig B_4 and dogfish A_4 isozymes of LDH exhibit an initial burst during the approach of pyruvate-enol (Pyr_E) to its steady-state level (Figure 1 of supplementary material; see paragraph concerning supplementary material at the end of this paper) as would be expected from an earlier analysis (Burgner & Ray, 1974). (This burst was not observed previously because a less sensitive assay, based on absorbance changes, was used.) The magnitude of the burst (10% of the total reaction in both cases), obtained by extrapolating the linear, second phase of the reaction back to zero time, corresponds to an initial enol concentration of 5×10^{-8} M, which compares reasonably well with the value of 8×10^{-8} M pyruvate enol estimated from the equilibrium constant for the enolization of pyruvate (4×10^{-6}, Burgner & Ray, 1974) and the initial pyruvate concentration (0.02 M). (The time constants for the burst phase are 0.04 and 0.06 s^{-1} for dogfish A_4 and pig B_4 isozymes, respectively.) Thus, free pyruvate enol is an obligatory intermediate in the adduct reaction under these conditions (Sugrobova et al., 1972; Burgner & Ray, 1974), and the reaction is largely a steady-state process, except for the initial burst phase, as was suggested previously (Burgner & Ray, 1974).

The Effect of NAD and Pyruvate Concentration on the Forward Adduct Reaction. The values of the observed first-order rate constant for the forward adduct reaction are nonlinear (concave downward) with respect to both pyruvate and NAD concentration ($[E_0] \ll [NAD]$ and $[Pyr]$) at pH 7 and high imidazole concentration (0.3 M). Double-reciprocal plots of the values of k^f_{obsd} against the concentration of *either* reactant (Figure 2) also are concave downward, although k^f_{obsd} appears to exhibit a saturation effect at an "infinite" reactant concentration with either reactant similar to that observed by Sugrobova et al. (1972). Analogous results also are obtained from measurements of the absorbance change at 325 nm and with pig B_4 LDH (not shown). An increase in the amount of the adduct complex present at $t \to \infty$ also is observed with increasing reactant concentrations (not shown); hence, formation of the adduct complex must be reversible. In fact, the process E·adduct → E·NAD + Pyr provides a quantitative rationale for the nonlinear saturation kinetics for k^f_{obsd}. Thus, the expression for k^f_{obsd} from Scheme II is given by eq 2, under the present conditions (see Appendix).

$$k^f_{obsd} = \frac{k_f[Pyr]}{1 + \frac{[Pyr]}{K_{pyr}} + \frac{K_{NAD}}{[NAD]}} + k_r \qquad (2)$$

Here K_{NAD} and K_{Pyr} are the (pH-dependent) dissociation constants for complexes with the stochiometry E·NAD and E·NAD·Pyr, respectively, while k_f and k_r are the apparent (pH dependent) second- and first-order rate constants for the forward and reverse adduct reactions (see the Appendix). The solid lines in Figure 2 were calculated from eq 2 and values of the constants in the legend, which were estimated by nonlinear regression analysis of the k^f_{obsd} values in the figure. The data correlation thus obtained validates the involvement of an E·NAD·Pyr complex in the reaction, but does not provide a distinction between the E·NAD·Pyr_E and E·NAD·Pyr_K complex. However, the E·NAD·Pyr_E complex, even if present at its equilibrium concentration, could account only for a small fraction of the two E·NAD·Pyr complexes based on the following relationships: (a) K_{Pyr_E} should be similar to K_{Lac} (since Pyr_E resembles lactate, structurally); (b) K_{Lac} appears to be somewhat larger than K_{Pyr_K} (cf., Warren, 1970, Table 3) so that $K_{Pyr_E} > K_{Pyr_K}$; (c) $[Pyr_E]/[Pyr_K] \approx 4 \times 10^{-6}$ (at equilibrium; Burgner & Ray, 1974); (d) $[E\text{·}NAD\text{·}Pyr_E]/[E\text{·}NAD\text{·}Pyr_K] \leq 4 \times 10^{-6}$ (since at equilibrium the ratio of these two complexes should be equal to $K_{Pyr_K}[Pyr_E]/K_{Pyr_E}[Pyr_K]$). Hence, K_{Pyr} in eq 2 must refer to the dissociation constant for E·NAD·Pyr_K and subsequently will be referred to as K_{Pyr_K}. Thus, the limiting value of k^f_{obsd} at infinite [Pyr] must be produced by saturating E·NAD with Pyr_K.

The following points provide further support for the claim that the relationship between k^f_{obsd} and the reactant concentrations in Figure 2 is adequately correlated by eq 2. (a) The

TABLE I: Values of Rate Constants for the Adduct Reaction Catalyzed by LDH.[a]

	Dogfish A_4	Pig B_4
k_2/k_5	0.4	0.4
k_4/k_5	2.7 s^{-1}	4.6 s^{-1}
$k_6 \times 10^3$	7.8	3.8
$k_1{}^b \times 10^{-5}$	3.0 $M^{-1} s^{-1}$	4.1 $M^{-1} s^{-1}$
$k_3{}^b$	0.2 $M^{-1} s^{-1}$	0.2 $M^{-1} s^{-1}$
$k_5/K_{Pyr_E}{}^b \times 10^5$	8.0 $M^{-1} s^{-1}$	9.4 $M^{-1} s^{-1}$

[a] The values of the constants described in Scheme I were obtained by regression analysis of the data in Figure 3; see the Results. [b] Calculated from the appropriate values in the upper half of this table and estimates for K_{eq}, 430 M^{-1}; K_{Pyr_K}, 0.013 M for dogfish A_4; K_{eq}, 990; K_{Pyr_K}, 0.005; and K_{enol}, 4×10^{-6} (Burgner & Ray, 1974) according to equations given in the Appendix.

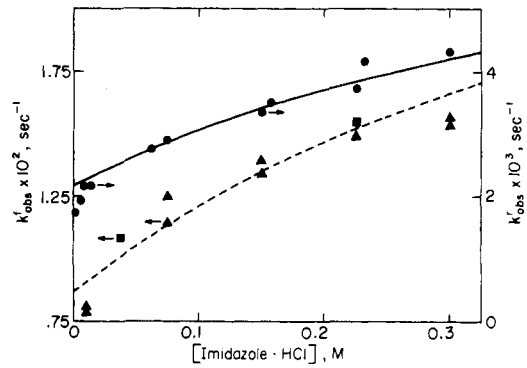

FIGURE 3: The effect of imidazole on the observed first-order rate constant for the forward and reverse adduct reaction. Values of k_{obsd} were obtained at pH 7 from transformed fluorescence–time curves (see Figure 1 and Results) by either graphical analysis for the reverse reaction (●) or nonlinear regression analysis for the forward reaction, according to eq 5 (Appendix) (▲); two other values of k^f_{obsd} (■) were calculated from spectroscopic data presented previously (Table I, Burgner & Ray, 1974). The fluorescence assay mixture for the forward reaction initially contained 4×10^{-3} M NAD, 0.02 M pyruvate, 2.5 to 4.0×10^{-7} M LDH at an ionic strength of 0.32, and that for the reverse reaction initially contained 1×10^{-4} M pyruvate, 2×10^{-4} M NAD, and 1.4×10^{-7} M E·adduct at an ionic strength of 0.3. Both assay mixtures contained NaCl and imidazole·hydrochloride such that the sum of their concentrations was 0.3 M. The other conditions are the same as those in Figure 1. The solid and dashed lines were obtained from functions describing Scheme II and the data in Table I (see the Results).

values of K_{NAD} obtained for dogfish A_4 LDH, 1.3 mM (from Figure 2), and for pig B_4 LDH, 0.3 mM (plot not shown), are similar to those obtained from kinetic studies with the dogfish enzyme, 0.4 mM (Burgner, 1973), and from equilibrium binding studies for the pig enzyme, 0.2 mM; Stinson & Holbrook, 1973). (b) The values of k_r—2.6×10^{-3} s^{-1} dogfish A_4; 2.3×10^{-3}, pig B_4—are essentially the same as those obtained by direct measurement of the reverse adduct reaction (see below): 3.3×10^{-3} s^{-1}, dogfish A_4; 2.0×10^{-3} s^{-1}, pig B_4. Unfortunately the value of K_{Pyr_K} is not well defined by the least-squares procedures used in the data fitting step, because pyruvate concentrations in excess of 0.02 M produce substantial inner filter effects in the fluorescence assay. Hence, the best estimates for K_{Pyr_K}—0.013 M, dogfish A_4; 0.005 M, pig B_4—are reported only because they are similar to lower limit values for this constant obtained from the normal enzymic reaction at high pyruvate concentrations: 0.01 M, dogfish, 0.001 M, pig (Burgner et al., 1978).

The Fate of the Adduct on Decomposition of the E·Adduct Complex. The E·adduct complex can decompose by either or both of two pathways: direct dissociation to give free enzyme and free adduct, or reversal of the formation process (see Scheme II). These two processes can be separated, since the *free* adduct exhibits a fairly intense absorption band with a maximum at 340 nm (Everse et al., 1971a), where neither NAD nor pyruvate adsorb significantly and where E·adduct absorbs only to a smaller extent. Hence, the fate of the adduct was examined by different spectroscopy (at pH 7 and 9) after diluting an equilibrium mixture of adduct complex and reactants by 34-fold into either 0.2 M NaCl or 0.1 M oxalate (which was used to ensure that the decomposition went to completion) plus either 0.3 M imidazole chloride or 0.3 M Tris-Cl. The results (see Figure 2 of supplementary material) indicate that at pH 7 at least 95% of the E·adduct complex reverts to starting materials via E·NAD·Pyr_E and E·NAD + Pyr (the reverse adduct reaction) either in the presence or absence of oxalate; i.e., no more than about 5% of the adduct complex dissociates directly to free adduct. (However, at pH 9 a much larger fraction of the decomposition involves direct dissociation of the adduct complex.)

The Second Buffer Effect. At low enzyme concentration, Pyr_E is at its equilibrium concentration during the adduct reaction, and a buffer effect on the enzyme-catalyzed adduct reaction under these conditions must involve some process other than the tautomerization of free Pyr_K. Such a buffer effect is demonstrated by plots of k_{obsd} against buffer concentration in Figure 3 for both the forward and reverse adduct reactions under such conditions and at constant ionic strength (maintained by use of KCl); similar results are obtained with pig B_4 LDH. (This effect also was noted previously for the forward reaction at relatively high enzyme concentration (Table I, Burgner & Ray, 1974)). Although the scatter in the value of the rate constants, thus obtained, is rather large relative to overall effect, the trends in the data are certainly real and can be rationalized in terms of a buffer-assisted tautomerization of *bound* pyruvate, E·NAD·Pyr_K ⇌ E·NAD·Pyr_E (cf., Scheme II). The solid lines in Figure 3 represent a numerical fit of the data to the expected equation for k^r_{obsd} according to Scheme II, viz., eq 3 where k^r_{obsd} is the observed rate constant for the reverse reaction under conditions where the reverse process goes to completion.

$$k^r_{obsd} = \frac{k_6(k_2 + k_4[B])}{k_2 + k[B] + k_5} \quad (3)$$

This equation requires a finite value of k^r_{obsd} at [B] → 0 and a hyperbolic increase to a new limiting value at [B] → ∞, as is suggested by the data (●). The estimated values for the constants k_6, k_2/k_5, and k_4/k_5 are given in Table I for both dogfish A_4 and pig B_4 LDH.

The forward adduct reaction was more difficult to follow accurately, and an analysis of its buffer dependence seemed unwarranted. However, to demonstrate the consistency of the approach used above, the expected values for k^f_{obsd} were calculated from eq 3 and 4 and the data in Table I—dashed line, Figure 3. Since values for the last three rate constants of Table I are calculated from the first three (see eq 7), this correlation of the observed data only demonstrates (a) that the estimated value of K_{eq} is in the right range (see below) and is independent of buffer concentration (as it should be) and (b) that eq 4, which is derived from Scheme II (see Appendix), adequately describes the relationship between k^r_{obsd} and k^f_{obsd}.

$$k^f_{obsd} = k_f[Pyr]\,(1 + K_{NAD}/[NAD] + [Pyr]/K_{Pyr_K})^{-1} + k_r \quad (4)$$

The similarity in the estimated value for the association con-

stant (k_1, Scheme II) for Pyr_E and E·NAD, 3×10^5 M^{-1} s^{-1}, at 15 °C, and the value for the analogous step in the normal enzymic reaction, the association of E·NAD and lactate, about 1.3×10^5 M^{-1} s^{-1} for pig B_4 LDH at 6.5 °C (Sudi, 1974), also seems worth noting.

Since the equation for k^f_{obsd} (eq 14, Appendix) contains separate terms for the flux through the alternative pathways to E·NAD·Pyr_E in Scheme II, the fraction of the total flux arising from the buffer assisted enolization of *bound* ketone can be calculated. This fraction, which is equal to $k_3[B]/(k_1K_{enol}K_{Pyr_K} + k_3[B])$, should become equal to 0.5 at approximately 0.16 M imidazole according to the data in Table I. In addition, the maximum size of buffer effect on k_{obsd} (i.e., the extent to which the buffer-assisted process E·NAD·Pyr_K → E·adduct contributes to the overall rate relative to E·NAD + Pyr_E → E·adduct) also can be expressed from eq 14 as the ratio $1 + k_5/k_1K_{Pyr_E}$; from the constants in Table I, this ratio is less than fourfold.

The Equilibrium Constant for the Adduct Reaction. At equilibrium, the amount of the adduct complex present is a function of [Pyr] and [NAD], and the expected relationship between the reciprocal fraction of the enzyme present as E·adduct, according to Scheme II, is given by eq 5 (assuming that the concentration of E·NAD·Pyr_E is negligible with respect to the other reactant species—see above—and that E·NAD + Pyr is in rapid equilibrium with E·NAD·Pyr_K; cf., Burgner et al., 1978).

$$\frac{E_t}{[\text{E·adduct}]} = 1 + \frac{1}{K_{eq}K_{Pyr_K}} + \frac{1}{K_{eq}[\text{Pyr}]}\left(1 + \frac{K_{NAD}}{[\text{NAD}]}\right) \quad (5)$$

Here K_{eq}, the (pH-dependent) equilibrium constant, is equal to [E·adduct]/[E·NAD][Pyr] (see also eq 7 and 13 in the Appendix; for definitions of the constants, see Scheme II). If the initial protein fluorescence of a reaction mixture (obtained by extrapolation of the decrease in fluorescence during the adduct reaction to $t = 0$) is F_i, the end-point fluorescence is F_∞, and the fluorescence of enzyme completely liganded with adduct is F_s, the equilibrium ratio, E_T/E·adduct, is proportional to $F_i^{1/4}/(F_i^{1/4} - F_\infty^{1/4})$. (The proportionality constant $(F_i^{1/4} - F_s^{1/4})/F_i^{1/4}$ must be determined independently (see below).) Although plots (not shown) for $F_i^{1/4}/(F_i^{1/4} - F_\infty^{1/4})$ against the reciprocal of the varied reactant concentration for either NAD or pyruvate are linear, the lines generated with pyruvate as the variable reactant do not intersect at a common point on the vertical axis as is required by eq 5—a 10% decrease in the vertical intercept value was observed for an eightfold increase in the NAD concentration (0.5 to 4 mM). The basis of this decrease is unknown; however, a small decrease in the fluorescence of E·NAD or E·NAD·Pyr_K complexes relative to E could be the cause.[3] Because the results of a limited study of this enzyme using absorbance measurements and a more extensive absorbance study with pig A_4 (Sugrobova et al., 1973) indicated a common vertical intercept when pyruvate is the varied reactant, and because the effect observed here was small, the data were scaled to a common vertical intercept based on that observed at highest NAD concentration used (4.0 mM). The estimate for K_{NAD}, obtained by using a nonlinear regression procedure to fit the scaled data to eq 5 in its reciprocal form, is 1 mM and is in reasonable agreement with that obtained under the same experimental conditions from the variation in k^f_{obsd} with [NAD] in Figure 2: 1.3 mM. To determine values for K_{eq} and K_{Pyr_K}, a value of 0.35 for the proportionality constant, $(F_i^{1/4} - F_s^{1/4})/F_i^{1/4}$, was estimated from the equilibrium ratio of 1.14 for E_t/E·adduct in 20 mM pyruvate and 4 mM NAD (ratio obtained with the initial velocity assay for E·adduct: Burgner et al., 1978) and that for $F_i^{1/4}/(F_i^{1/4} - F_\infty^{1/4})$ under the same conditions, 3.26. A value for K_{eq} of 350 M^{-1}, which compares reasonably well with that (430 M^{-1}) obtained from the ratio of k_f to k_r, was then calculated from the regression coefficient for the fit of the data to eq 5 and the above proportionality constant. Thus, site occupancy is reasonably expressed by eq 4; although under the conditions used the term, $(K_{eq}K_{Pyr_K})^{-1}$, was not significantly different from zero.

Substrate Specificity of the Enzymic Adduct Reaction. Of the potential reactants that were tested for their ability to function in the adduct reaction, only fluoropyruvate reacted at a rate (2.4×10^{-3} s^{-1}) somewhat comparable to that for pyruvate (1.5×10^{-2} s^{-1}) while α-hydroxypyruvate showed only slight activity relative to pyruvate (about 0.1%), and the inactive substrates are bromopyruvate, α-ketobutyrate, acetone, and acetaldehyde. (The assay contained 5×10^{-6} M dogfish LDH, 4×10^{-3} M NAD, 0.3 M imidazole chloride, pH 7, and 0.02 M ketone, except for acetone, which also was used at 1.0 M.)

Discussion

The results of the present study of the LDH-catalyzed adduct reaction are summarized by the reaction pathway in Scheme II. Although this scheme is more complex than that considered previously (Burgner & Ray, 1974), the additional steps in no way invalidate the previous study, which was conducted under a more limited set of conditions. The new evidence about the mechanism of the adduct reaction is summarized below.

The involvement of free pyruvate enol as an intermediate in the adduct reaction (previously inferred from the similarity of the buffer-dependent rate constants for the adduct reaction and for the iodination of pyruvate (Burgner & Ray, 1974)) is now confirmed by the observation of a small, pre-steady-state burst phase at low buffer concentration that corresponds to the initial concentration of enol present in the reaction (about 8×10^{-8} M at 0.02 M pyruvate). Hence, during the course of most of the adduct reaction at low buffer and intermediate enzyme concentration, pyruvate enol reacts with the enzyme (E·NAD) to produce the adduct complex as fast as the enol is formed (Burgner, 1973). Thus, the suggestion of Sugrobova et al. (1972), that the ternary complex E·NAD·Pyr_E is at equilibrium with respect to E·NAD plus pyruvate, and that the adduct is formed relatively slowly from E·NAD·Pyr_E, no longer is tenable. The saturation kinetics observed in the adduct reaction when the pyruvate concentration is increased and when $Pyr_K \rightleftharpoons Pyr_E$ is at equilibrium (Figure 2) is caused by the equilibrium formation of the less reactive E·NAD·Pyr_K complex. In addition, the reverse adduct reaction (k_6, Scheme II), which, at pH values less than about 9, is substantially faster than direct dissociation to E + adduct (cf., Arnold & Kaplan, 1974), is required both by kinetic and equilibrium processes. Finally, both kinetic and equilibrium studies confirm the equality and independence of the four active sites in dogfish A_4 LDH, in accord with the conclusions of Stinson & Holbrook (1973).

[3] Both F_i and F_∞ in the expression $F_i^{1/4}/(F_i^{1/4} - F_\infty^{1/4})$ are equal to the sum of the $Q_n[E_n]$ terms where Q_n is the fluorescence coefficient and $[E_n]$ the concentration of the enzymic species, E, E·NAD·Pyr_K, and E·adduct. In fact, F_i and F_∞ can be used to calculate $[E_t]$/[E·adduct] only if the Q_n values for the first three of the above species are approximately the same, viz., so that $Q_E[E] + Q_{E\text{·}NAD}[E\text{·}NAD] + Q_{E\text{·}NAD\text{·}Pyr}[E\text{·}NAD\text{·}Pyr] = Q_R[E_R]$. Since the fluorescence lifetimes of the tryptophans in all three species are the same (within an error margin of ±10%: J. W. Burgner II, unpublished results), this approximation should be sufficient for the purposes of this study.

These considerations provide ample support for the steps in the adduct reaction formulated in Scheme II, except for the step associated with the rate constants, k_3 and k_4 (see below). In addition, the reaction sequence involving free Pyr_E is shown to be analogous to the normal enzymic oxidation of lactate in terms of (a) the order in which the reactants add, (b) the rapidity of the bond-forming process which reduces the concentration of the competent ternary complex to insignificant levels, (c) the reversibility of the bond-forming step, and (d) the nature of the chemical process, viz., "carbanion" transfer and "hydride" transfer, respectively.

The increased rate of the adduct reaction produced by the "second" buffer effect (cf., Burgner & Ray, 1974) occurs under conditions where the "first" buffer effect no longer affects the rate, because the process $Pyr_K \rightleftharpoons Pyr_E$ is *at equilibrium*. Although this second buffer effect is not very large and is difficult to quantitate, experimentally, because at high buffer concentration another step becomes rate limiting (see the Results), it is certainly real and can be observed in both the reverse as well as the forward reactions (see the Results). Since the first buffer effect is related to the rate of formation of Pyr_E and thus to the rate of formation of E·NAD·Pyr_E from E·NAD and free Pyr_E, the above considerations require that the adduct reaction be formulated either (a) so that the second buffer effect is involved in a *subsequent reaction* of E·NAD·Pyr_E, i.e., a *sequential buffer effect* occurs (see Scheme III) or (b) so that

SCHEME III

$$E + NAD^+ \underset{K_{NAD}}{\rightleftharpoons} [E\cdot NAD]$$

$$+ \left[\begin{array}{c} Pyr_E \\ k_e[B] \Big\| k_K[B] \\ Pyr_K \end{array}\right] \underset{k_2}{\overset{k_1}{\rightleftharpoons}} E\cdot NAD\cdot Pyr_E \underset{k_6 + k_6'[B]}{\overset{k_5 + k_6'[B]}{\rightleftharpoons}} E\cdot adduct$$

$$\left[\begin{array}{c} Pyr_K \end{array}\right] \underset{K_{Pyr_K}}{\rightleftharpoons} E\cdot NAD\cdot Pyr_K$$

at a *parallel pathway* for the formation of E·NAD·Pyr_E, viz., E·NAD·Pyr_K → E·NAD·Pyr_E is included, i.e., a *parallel buffer effect* occurs (see Scheme II). There are three reasons for choosing the parallel pathway instead of the subsequent reaction sequence. Thus, it is unlikely that an *external* base could facilitate the adduct reaction by acting on the enolic hydroxyl group in E·NAD·Pyr_E, since buffer-assisted proton removal from hydroxyl groups is not observed in aqueous solution, and since the involvement of an *external* base in this system would require that the hydroxyl group in question be in a largely aqueous environment. In addition, the enolization of pyruvate in the E·NAD·Pyr_K complex *should* occur, unless steric factors preclude access of a base to the C_3 hydrogens of bound pyruvate, since E·NAD·Pyr_E is a viable complex. That at least one of these C_3 hydrogens is in a fairly accessible position is indicated by the undiminished binding to E·NADH of pyruvate analogs with bulky substituents at the 3-carbon, coupled with their definite (although substantially reduced) reactivity in the normal enzymic process, e.g., *o*-nitrophenylpyruvate (Holbrook & Stinson, 1973). Finally, the following arguments show that the rate of the adduct reaction varies with the concentration of LDH in accord with the parallel pathway (Scheme II) and not the sequential pathway (Scheme III).

Equation 16 (Appendix) specifies the time course of the Scheme II reaction as a function of initial conditions. At low buffer concentrations and at saturating NAD, the initial rate of the adduct reaction should be a complex function of enzyme concentration. This is shown in the Figure 4 log-log plot (—)

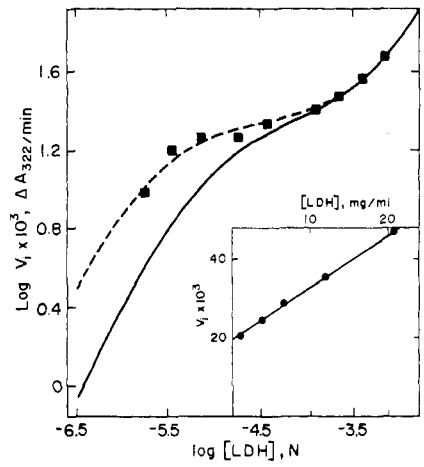

FIGURE 4: A log-log plot of the initial velocity of the adduct reaction against the concentration of pig heart LDH. The initial velocities in this figure, from the Ph.D. thesis of C. C. LoBue (1971, Figure 16), were obtained in the presence of 0.05 M phosphate, pH 7.0 at 23 °C with a spectral assay similar to that described in the Experimental Section and at reactant concentrations of 9.5×10^{-4} M NAD and 9.5×10^{-3} M pyruvate. Both lines in this figure were calculated with eq 16. For the dashed line, values of the rate constants obtained with the pig B enzyme at 15 °C—$k_1 = 4 \times 10^5$ M^{-1} s^{-1}, $k_2 = 9.6 \times 10^3$ s^{-1}, $k_5 = 2.5 \times 10^5$ s^{-1}, $K_{enol} = 4 \times 10^{-6}$ (Table I); at 23 °C; 0.05 M phosphate, $k_k[B] = 1.2$ s^{-1}, $k_4[B] = 138$ (J. W. Burgner, II, unpublished results)—were used; a value for $k_3[B]/K_{Pyr_K} = 2.2 \times 10^{-2}$ M^{-1} s^{-1} also was used (see below). The solid line, k_1, was increased to 1.6×10^5 M^{-1} s^{-1}, and $k_4[B]$ decreased to 76 s^{-1} (see the Discussion). (Inset) A plot of initial velocity against LDH concentration for the five highest enzyme concentrations in the main figure. Intercept and slope values of $1.95 \pm 0.1 \times 10^{-2}$ ΔA_{322} min^{-1} and $1.31 \pm 0.02 \times 10^{-3}$ ΔA_{322} min^{-1} mg^{-1}, respectively, were estimated by least-squares analysis, and the solid line reflects these values. From the regression coefficients, $k_e[B]$ is calculated as 4.4×10^{-6} s^{-1} and $k_3[B]/K_{Pyr_K}$ as 2.2×10^{-2} M^{-1} s^{-1} from eq 15 by assuming that $k_4[B]$ was negligible with respect to k_5 (see above).

which was calculated from eq 16 by use of the constants in Table I for pig B_4. In the lowest concentration range (the lower, left-hand limb of the curve), the initial rate is nearly a linear function of $[E_0]$, the process $Pyr_K \rightleftharpoons Pyr_E$ is almost at equilibrium, and the rate-determining step is the formation of the weak E·NAD·Pyr_E complex. In the intermediate range (the plateau region), the concentration of E·NAD is sufficiently high that Pyr_E binds to and reacts with the enzyme as fast as it is formed, so that the reaction becomes zero order in enzyme concentration. At still higher enzyme concentrations, the parallel reaction E·NAD·Pyr_K → E·NAD·Pyr_E begins to compete with the above process; E·NAD·Pyr_K predominates so that the reaction again becomes a linear function of enzyme concentration. The absence of the upper limb is the only kinetic feature that distinguishes the sequential pathway of Scheme III from the parallel pathway of Scheme II. (The rate equation for Scheme III is given in the supplementary material.)

The lower limb and plateau regions of the adduct reaction have been described previously (Burgner & Ray, 1974) and further verified in the present paper for both the dogfish and pig heart enzymes. In addition, data from the Ph.D. thesis of C. C. LoBue (1971) clearly show all three phases of the adduct reaction. Thus, from a qualitative standpoint, the dependence of the rate of the adduct reaction on enzyme concentration is consistent with the parallel pathway of Scheme II.

The following quantitative comparisons also can be made. In Figure 4 the dashed line shows a fit of eq 15 to LoBue's data that was obtained by making minor alterations in the constants that we measured with the pig heart enzyme. Since the reaction temperature was 7 °C higher and phosphate was used as the buffer instead of imidazole, the changes in the various con-

stants required to obtain this fit seem reasonable (see figure legend). In addition, the linear dependence of the rate of adduct formation on the concentration of enzyme in the high concentration range that is expected from Scheme II (see above) is shown by plot in the inset of Figure 4. The involvement of parallel pathways for formation of the adduct complex from E·NAD and Pyr_K thus seems adequately verified. In discussing her results LoBue suggested this mechanism, among others, as a possible qualitative rationale for her data.

The reaction, E·NAD·Pyr_K → E·NAD·Pyr_E, is unique[4] in that an *external*, i.e., nonenzymic, base is involved in an enzymic process where the enzyme undoubtedly acts as a general acid by donating a proton to the keto group of E·NAD·Pyr_K. In fact, a preliminary estimate of 1400-fold for the rate enhancement by the enzyme for this process can be obtained from the value for k_3 in Table I (0.2 M^{-1} s^{-1}) and that for the analogous nonenzymic process catalyzed by imidazole (1.4×10^{-4} M^{-1} s^{-1}; Burgner & Ray, 1974). Moreover, a comparison of the reverse of this process, the (general) acid-catalyzed, enzyme-facilitated ketonization of bound Pyr_E, with the nonenzymic process catalyzed by the same general acid should allow an assessment of the extent to which general base catalysis of LDH facilitates not only the adduct reaction but also the normal LDH-catalyzed oxidation of lactate, because of the similarities in the two processes (see above). An assessment of this and of other aspects of the role of LDH in the oxidation of lactate based on comparisons between the LDH catalyzed and the nonenzymic adduct reactions will be made in a subsequent paper.

Appendix

The steady-state rate equation for the adduct reaction in Scheme II, under conditions where dissociation of E·adduct is insignificant (pH 6 to 8), was formulated by assuming that the concentration of E·NAD·Pyr_E was negligible with respect to that of the other enzyme species. In such a case, the conservation equation for Scheme II becomes

$$E_T = E + E\cdot NAD + E\cdot NAD\cdot Pyr_K + E\cdot adduct$$

If the sums of E, E·NAD, and E·NAD·Pyr_K are considered as reactant forms of the enzyme, E_R

$$E_T = E_R + E\cdot adduct$$

If, in addition, both $d[Pyr_E]/dt$ and $d[E\cdot NAD\cdot Pyr_E]/dt$ are taken as much smaller than $d[E\cdot adduct]/dt$, the following differential equation for disappearance of the reactant forms of the enzyme can be formulated.

$$\frac{d[E_R]}{dt} = -\{f(NAD,Pyr) + K_{eq}[Pyr]\}k_5 \times \frac{(k_3[B]/K_{Pyr_K} + k_1\Pi_t K_{enol})([E_R]_t - [E_R]_\infty)}{f(NAD,Pyr)K_{eq}[k_2\Pi_t + k_4 + k_5]} \quad (6)$$

The subscripts 0, t, and ∞ refer to reaction times; the following relationships also hold:

$$K_{eq} = \frac{k_5 K_{enol}}{k_6 K_{Pyr_E}} = \frac{k_3 k_5}{k_4 k_6 [K_{Pyr_K}]} \quad (7)$$

$$\Pi_t = k_k[B]/\{k_k[B] + k_1[E_R]_t f(NAD,Pyr)^{-1}\} \quad (8a)$$

The partition expression for Pyr_E, Π_t, is related to the relative concentrations of E_R, and thus changes with time; it becomes equal to Π_0 or Π_∞ at $t = 0$ or $t \to \infty$, viz., when $[E_R]_t$ is equal to $[E_R]_0$ or $[E_R]_\infty$.

$$f(NAD,Pyr) = 1 + K_{NAD}/[NAD] + [Pyr]/K_{Pyr_K} = [E_R]/[E\cdot NAD]$$

Although eq 6 cannot be integrated to give $[E_R]_t$ as a function of t, it can be arranged and integrated (by standard procedures) to give t as a function of $[E_R]_t$. Equation 9 is obtained in this manner, after evaluating the integration constant (by setting $[E_R]_t = [E_R]_0$) and defining a recurring collection of constants:

$$\theta = k_1 K_{enol} K_{Pyr_K}/k_3[B] = k_2/k_4[B] \quad (8b)$$

$$t = \frac{K_{eq} f(NAD,Pyr)}{f(NAD,Pyr) + K_{eq}[Pyr]}\left\{\frac{1}{k_f}\ln\frac{[E_R]_0 - [E_R]_\infty}{[E_R]_t - [E_R]_\infty} + \frac{K_{Pyr_K}\theta\Pi_\infty}{k_3[B](1 + \theta\Pi_\infty)}\ln\frac{1 + 1/\theta\Pi_0}{1 + 1/\theta\Pi_t}\right\} \quad (9)$$

Here, k_f is given by the following expression

$$k_f^{-1} = (k_5 k_{enol}/K_{Pyr_E})^{-1} + \{(1 + \theta\Pi_\infty)k_3[B]/K_{Pyr_K}\}^{-1} \quad (10)$$

Equation 9 can be simplified for three limiting cases, two of which were considered in a previous paper (Burgner & Ray, 1974), although the latter two cases will be obtained directly from eq 6. These cases are readily defined in terms of two partition functions, Π (eq 8a) and θ (eq 8b). The expression for Π can be rewritten as

$$\Pi = k_k[B]/\{k_k[B] + k_1[E\cdot NAD]\} \quad (11)$$

and this is equal to the fraction of Pyr_E that returns to Pyr_K. The fate of E·NAD·Pyr_E relative to dissociation (to give Pyr_E) and ketolization (to give E·NAD·Pyr_K) is given by θ (see eq 8b).

The first case involves conditions where the reaction is first order in disappearance of the reactant forms of the enzyme, E_R. Under these conditions, Pyr_E is at its equilibrium concentration, $k_k[B] \gg k_1[E\cdot NAD]$, Π is equal to unity, and the second logarithmic term in eq 9 disappears. Hence

$$\ln\frac{[E_R]_0 - [E_R]_\infty}{[E_R]_t - [E_R]_\infty} = k^f_{obsd}t$$

where

$$k^f_{obsd} = k_f\left\{\frac{f(NAD,Pyr) + K_{eq}[Pyr]}{K_{eq}f(NAD,Pyr)}\right\} \quad (12)$$

or

$$k^f_{obsd} = k_f[Pyr]/f(NAD,Pyr) + k_r$$

and where

$$K_{eq} = k_f/k_r \quad (13)$$

Under these conditions the expression for the rate constant in the forward reaction (eq 10) reduces to

$$k_f^{-1} = (k_5 K_{enol}/K_{Pyr_E})^{-1} + (k_1 K_{enol} + k_3[B]/K_{Pyr_K})^{-1} \quad (14)$$

Under *initial* conditions, the second and third cases occur, respectively, at "intermediate" enzyme concentrations where the reaction is zero order in enzyme and at "high" enzyme concentrations where the reaction is again first order in enzyme. Both cases require that E·NAD react with Pyr_E as fast as it is formed, i.e., $k_1[E\cdot NAD] \gg k_k[B]$ so that Π equals

[4] A buffer-assisted migration of a proton between two ionizable groups during the carbonic anhydrase cycle (cf., Tu & Silverman, 1977) apparently is the closest analogy to the present buffer effect.

$k_k[B]/k_1[E\cdot NAD]$. In addition, the inequality $k_2\Pi \ll k_4[B] + k_5$ must be valid. Under these restrictions, eq 6 reduces to the following expression

$$\frac{d[E_R]}{dt} = -\frac{k_5}{(k_4[B] + k_5)} \times \left\{k_e[B][Pyr] + \frac{k_3[B][E_t][Pyr]}{K_{Pyr_K} f(NAD,Pyr)}\right\} \quad (15)$$

The first and second terms within the braces describe, respectively, components that are zero order and first order in enzyme; the coefficient $k_5/(k_4[B] + k_5)$ describes the partition of $E\cdot NAD\cdot Pyr_E$ between product and reactants. (The integrated form of eq 15 also can be obtained from eq 9 by suitable manipulations.) Hence, under appropriate conditions, a reaction that proceeds according to Scheme II will appear first order in enzyme at low enzyme concentration, zero order at intermediate levels, and first order, again, at high levels.

Equation 6, under initial conditions and at reactant levels where the process approaches completion, becomes:

$$\frac{d[E_R]_{t\to 0}}{dt} = -\frac{k_5(k_3[B]/K_{Pyr_K} + k_1\Pi_0 K_{enol})\,[E_t][Pyr]}{(k_2\Pi_0 + k_4[B] + k_5) f(NAD,Pyr)} \quad (16)$$

Supplementary Material Available

Supplemental figures (1 and 2) and rate equation for Scheme III (7 pages). Ordering information is given on any current masthead page.

References

Arnold, L. J., Jr., & Kaplan, N. O. (1974) *J. Biol. Chem. 249,* 652.

Burgner, J. W., II (1973) Ph.D. Thesis, Purdue University, West Lafayette, Ind.

Burgner, J. W., II, & Ray, W. J., Jr. (1974) *Biochemistry 13,* 4229.

Burgner, J. W., II, Ainslie, G. R., Jr., Cleland, W. W., & Ray, W. J., Jr. (1978) *Biochemistry 17* (preceding paper in this issue).

DiSabato, G. (1968) *Biochem. Biophys. Res. Commun. 33,* 688.

Everse, J., Barnett, R. E., Thorne, C. J. R., & Kaplan, N. O. (1971a) *Arch. Biochem. Biophys. 143,* 444.

Everse, J., Zoll, D. C., Kahan, L., & Kaplan, N. O. (1971b) *Bioorg. Chem. 1,* 207.

Griffin, J. H., & Criddle, R. S. (1970) *Biochemistry 9,* 1195.

Holbrook, J. J. (1972) *Biochem. J. 128,* 921.

Holbrook, J. J., & Gutfreund, H. (1973) *FEBS Lett. 31,* 157.

Holbrook, J. J., & Stinson, R. A. (1973) *Biochem. J. 131,* 739.

LoBue, C. C. (1971) Ph.D. Thesis, University of California, Davis, Calif.

Novoa, W. B., Winer, A. D., Glaid, A. J., & Schwert, G. W. (1959) *J. Biol. Chem. 234,* 1143.

Stinson, R. A., & Holbrook, J. J. (1973) *Biochem. J. 131,* 719.

Sudi, J. (1974) *Biochem. J. 139,* 261.

Sugrobova, N. P., Kurganov, B. I., Gurevich, V. M., & Yakoviev, V. A. (1972) *Mol. Biol. 8,* 716.

Sugrobova, N. P., Kurganov, B. I., & Yakoviev, V. A. (1973) *Mol. Biol. 6,* 217.

Tu, C. K., & Silverman, D. N. (1977) *J. Am. Chem. Soc. 99,* 2263.

Warren, W. A. (1970) *J. Biol. Chem. 245,* 1675.

Wassarman, P. M., & Lentz, P. J. (1971) *J. Mol. Biol. 60,* 509.